ORGANOMETALLICS
Article

Organometallics **2010,** *29,* 2521–2532 2521
DOI: 10.1021/om100131t

Online Monitoring of Hydroformylation Intermediates by ESI-MS

Christian H. Beierlein and Bernhard Breit*

Institut für Organische Chemie und Biochemie and Freiburg Institute for Advanced Studies (FRIAS), Albert-Ludwigs-Universität Freiburg, Albertstrasse 21, 79104 Freiburg, Germany

Roberto A. Paz Schmidt and Dietmar A. Plattner*

Institut für Organische Chemie und Biochemie, Albert-Ludwigs-Universität Freiburg, Albertstrasse 21, 79104 Freiburg, Germany

Received February 19, 2010

Self-assembling ligands bearing permanently charged moieties have been synthesized and investigated in the Rh-catalyzed hydroformylation of terminal alkenes. By coupling a high-pressure autoclave directly to an ESI mass spectrometer hydroformylation reactions applying self-assembling 6-DPPon ligands could be studied in an online fashion. The live-streaming of the reaction mixture to the spectrometer revealed a series of different complexes not observed by other methods before, the structures of which were corroborated by CID experiments. Under CO/H_2 atmosphere, new complexes that are predicted by the Wilkinson catalytic cycle could be identified and studied by CID experiments, too. Especially the ion at m/z 848, a square-planar hydrido-carbonyl complex that is normally not detectable by other methods, was investigated in detail. Collision experiments of this complex resulted in the loss of CO and H_2, the latter being quite unusual, and points to the involvement of the hydrogen bond framework. These findings were further supported by deuteration experiments that revealed a clear incorporation of deuterium into the ligands. From these findings a new hydrogen-activation mechanism was proposed. Furthermore, substrate-containing complexes could be generated too, though a huge excess of substrate was necessary. CID experiments either with D_2 or Ar yielded nearly identical spectra, hinting at a complex that might result either from a *β-hydride elimination* or from intramolecular *oxidative addition* of one of the ligands.

Introduction

In times of dwindling resources, transition-metal-catalyzed transformations are more and more a focus of common interest, enabling otherwise time- and energy-consuming processes in much milder and cost-efficient ways. A thorough understanding of the course and mechanism of these chemical reactions is of profound importance for improving catalysts and catalytic transformations by identifying reactivity- and selectivity-controlling interactions, intermediates, and transition states. However, due to the often unstable and short-lived nature of those species of interest, detection can be a tedious and time-consuming endeavor, applying, for example, isotope-labeling experiments. Thus, online methods that enable the direct observation of an ongoing reaction like IR and NMR techniques are commonly used nowadays. Unfortunately, specialized equipment is needed in most cases and the setup tends to be complicated and limited to only a handful of reactions, in addition to high ownership costs (e.g., ReactIR). The required accuracy for detection of intermediate species in low concentrations is often not met, thus rendering the methodology useless for online experiments. Because of the ease of transferring solution-phase ions to the gas phase for identification or further reactions, electrospray ionization mass spectrometry (ESI-MS) has become increasingly popular as a mechanistic tool for studying short-lived reactive intermediates in organometallic catalytic cycles.[1,2] Extending the previous applications to investigate chemical processes under pressure by ESI-MS, a setup for the direct coupling of a high-pressure autoclave to an electrospray tandem mass spectrometer was

Scheme 1. DNA Base Pair Inspired Self-Assembling Ligands

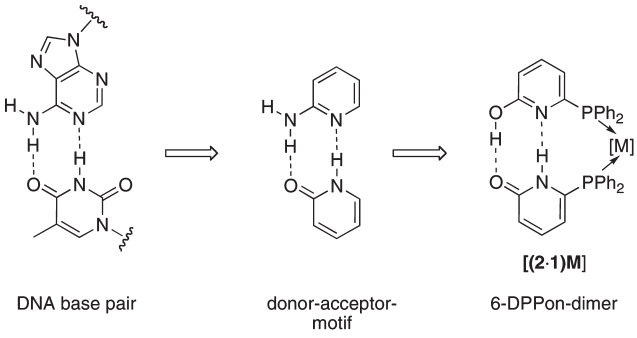

---

[1] Plattner, D. A. *J. Mass Spectrom.* **2001**, *207*, 125, and references therein.

[2] Plattner, D. A. *Top. Curr. Chem.* **2003**, *225*, 153, and references therein.

*Corresponding authors. E-mail: bernhard.breit@chemie.uni-freiburg.de; dietmar.plattner@chemie.uni-freiburg.de.

Scheme 2. Synthesis of 2

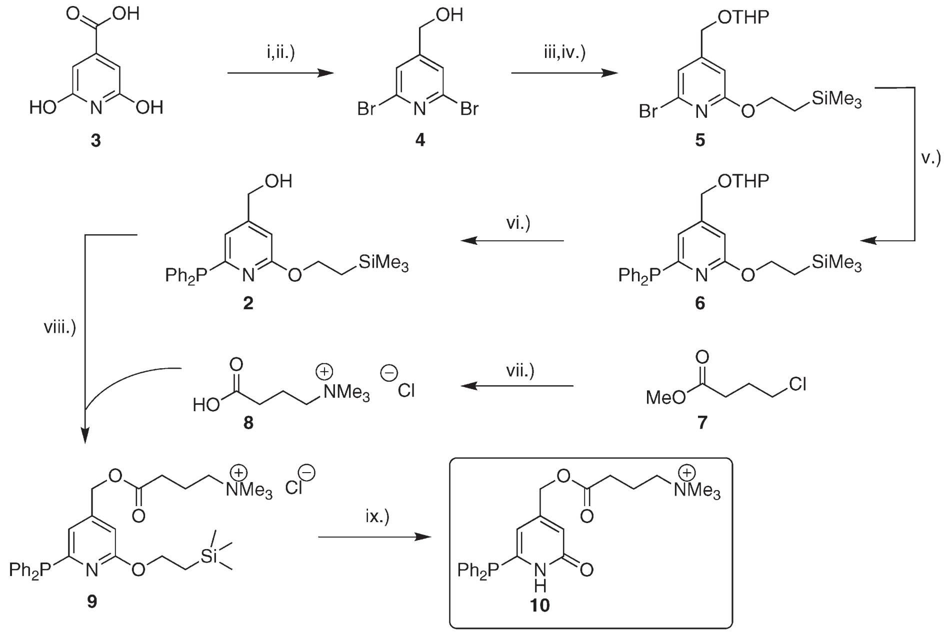

conditions: i.) POBr$_3$, 140 °C, 16h, 86%; ii.) NaBH$_4$, BF$_3$·OEt$_2$, THF, 0 °C RT, 99%; iii.) DHP, PPTS, CH$_2$Cl$_2$, RT, 16 h, 96%; iv.) NaH, HOCH$_2$CH$_2$SiMe$_3$, THF, RT, 16 h, 81%; v.) *n*-BuLi, Ph$_2$PCl, THF, -100 °C, 83%; vi.) MM K10, MeOH/THF, 55 °C, 91%; vii.) NMe$_3$ (30% *w/v*), acetone, RT, 72 h; 6 M HCl, 60%; viii.) DCC/DMAP, CH$_3$CN, RT, 20 h, ca.90%; ix.) TFA/DCM (1:10), RT, 30 min, 40%.

Scheme 3. ESI-MS Spectrum of 10 in CH$_3$CN

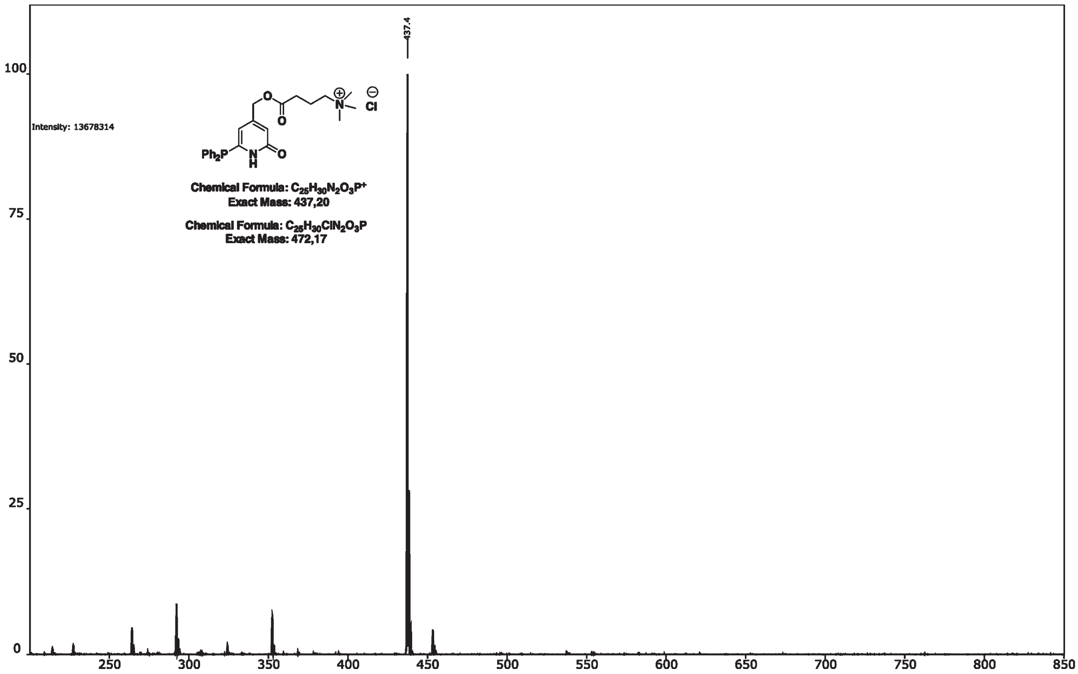

described recently.[3] This intriguing feature prompted us to have a closer look into the Rh-catalyzed hydroformylation of terminal alkenes,[4] one of the most important industrial applied transition-metal-catalyzed reactions and, by the definition of Trost,[5] a truly atom-economic transformation. Recently, Krische and co-workers demonstrated the unique advantages of ESI-MS for mechanistic studies on the related coupling of acetylene to carbonyl compounds.[6]

As the preparation of bidentate ligands often incorporates elaborate multistep syntheses, one of us introduced the concept of self-assembling ligands that mimic a bidentate binding motif in the presence of a transition metal (Scheme 1).[7,8] By simple mixing two monodentate ligands bearing a complementary hydrogen bond donor–acceptor motif, bidentate ligands can be formed in a combinatorial fashion. Attractive hydrogen-bond interactions of the donor–acceptor or acceptor–donor counterparts further stabilize the resulting complexes, which were successfully

---

(3) Paz Schmidt, R. A.; Plattner, D. A. *Anal. Chem.* **2009**, *81*, 3665.

Scheme 4. ^{31}P NMR Spectrum of 11

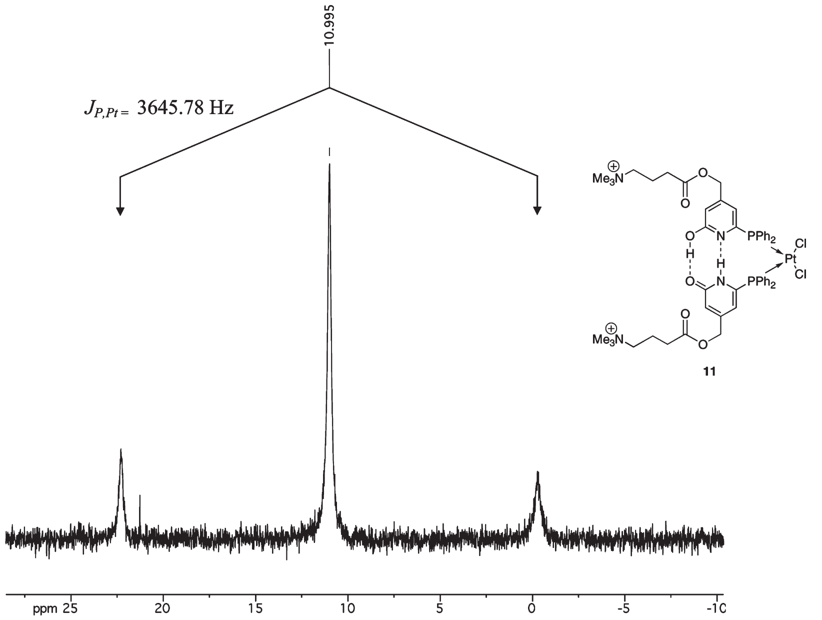

Scheme 5. ^1H NMR spectrum of 11

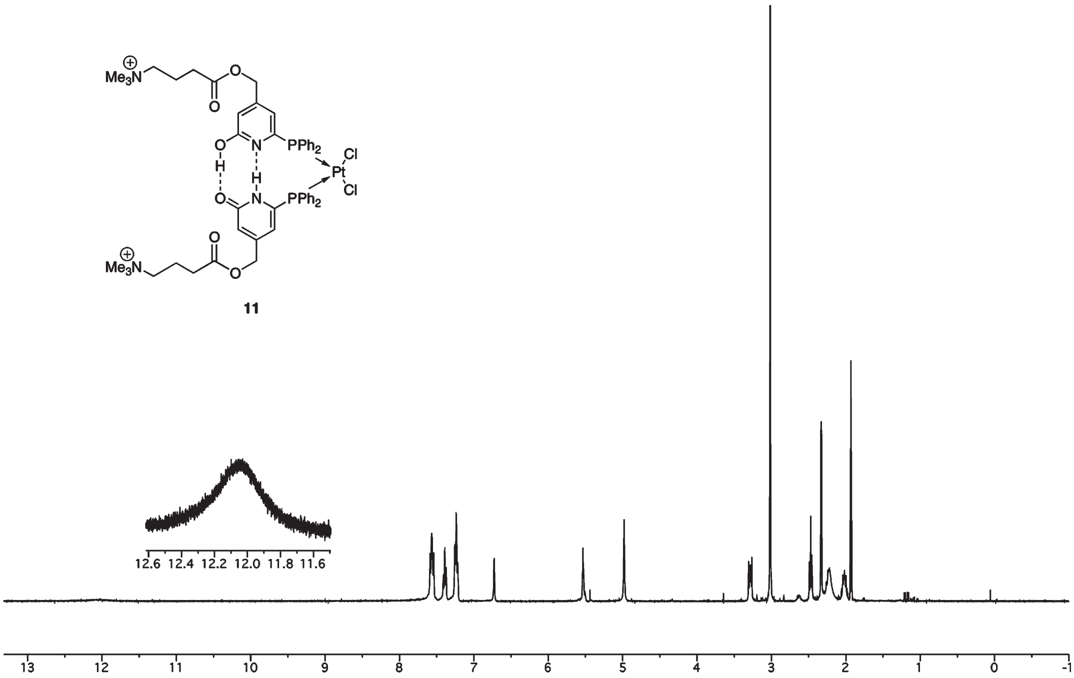

applied in a wide range of chemical transformations, e.g., rhodium-catalyzed regioselective hydroformylation of terminal

Table 1. Hydroformylation of 1-Octene Applying 10, 6-DPPon, and Mixtures of Ligands[a]

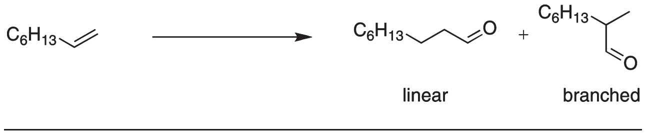

entry	solvent	ligand	conv (%)	selectivity (l:b)
1	CH_3CN	6-DPPon	100	93:7
2	CH_3CN	**10**	100	94:6
3[b]	CH_3CN	6-DPPon/**10** (1:1)	100	95:5
4	toluene	6-DPPon	100	97:3

[a] Conditions: Rh:L:1-octene = 1:10:500, *c*(1-octene) = 0.36 M, CO/H_2 (1:1), 10 bar, 70 °C, 20 h. [b] Rh:L1:L2:1-octene = 1:5:5:500, *c*(1-octene) = 0.36 M, CO/H_2 (1:1), 10 bar, 70 °C, 20 h.

---

(4) For selected reviews on alkene hydroformylation, see: (a) Cornils, B.; Herrmann, W. A.; Kohlpaintner, C. W. Otto Roelen as the Pioneer of Industrial Homogeneous Catalysis. *Angew. Chem., Int. Ed. Engl.* **1994**, *33*, 2144. (b) Beller, M.; Cornils, B.; Frohning, C. D.; Kohlpaintner, C. W. Progress in Hydroformylation and Carbonylation. *J. Mol. Catal.* **1995**, *104*, 17. (c) Frohning, C. D.; Kohlpaintner, C. W. In *Applied Homogeneous Catalysis with Organometallic Compounds*, Vol. *1*; Cornils, B.; Herrmann, W. A., Eds.; Wiley-VCH: Weinheim, 1996; pp 29−104. (d) Nozaki, K. In *Comprehensive Asymmetric Catalysis*; Jacobsen, E. N., Pfaltz, A., Yamamoto, H., Eds.; Springer-Verlag: Berlin, 1999; Vol. *1*, pp 381−413. (e) Breit, B. Synthetic Aspects of Stereoselective Hydroformylation. *Acc. Chem. Res.* **2003**, *36*, 264. (f) van Leeuwen, P. W. N. M. *Homogeneous Catalysis: Understanding the Art*; Kluwer: Dordrecht, 2004. (g) Breit, B. Recent Advances in Alkene Hydroformylation. *Top. Curr. Chem.* **2007**, *279*, 139.

(5) Trost, B. M. *Science* **1991**, *254*, 1471.

Scheme 6. ESI-MS Spectrum of 10 and $[Rh(NBD)_2]BF_4$ in CH_3CN (*m*/*z* 200−1200)

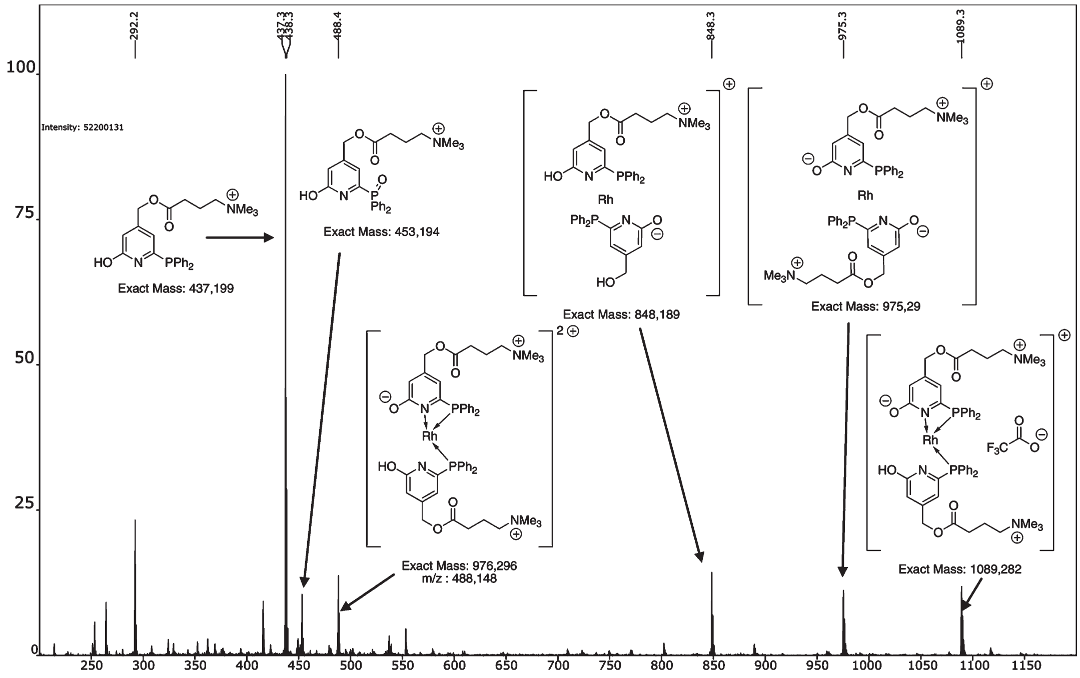

alkenes,[9] ruthenium-catalyzed anti-Markovnikov hydration of terminal alkynes,[10] rhodium-catalyzed asymmetric hydrogenation,[11] and nickel-catalyzed hydrocyanation of styrenes.[12]

The depicted 6-DPPon ligand **1** can be seen as the seminal example of our self-assembling ligands and holds an exceptional position, as it can act either as a hydrogen-donor−acceptor or hydrogen-acceptor−donor ligand by fast tautomerization between the pyridone and the hydroxypyridine form.[9] Though this self-complementarity impairs its applicability in the combinatorial generation of bidentate ligands, one has to synthesize only one monodentate ligand to generate bidentate ligands. Bearing this in mind, we have chosen the 6-DPPon platform as a model system for this mechanistic study.

Experimental Part

Ligand Synthesis. As only charged species can be detected by means of ESI-MS, we had to ensure that at any time in the catalytic cycle the intermediates of interest bear either a positive or a negative charge. Hence, we prepared the 6-DPPon derivative **2**, bearing an additional hydroxymethylene- moiety for further functionalization, e.g., through esterification with a charged carboxylic acid. This substitution pattern was chosen to ensure minimal interaction between the additional functional group and the hydrogen-bond network. Following literature precedence,[13] we decided to introduce a quaternary amine as a functional group with a permanent positive charge, which

Scheme 7. Catalytic Cycle for the Rhodium-Catalyzed Hydroformylation of 1-Hexene with the Masses of Expected Complexes

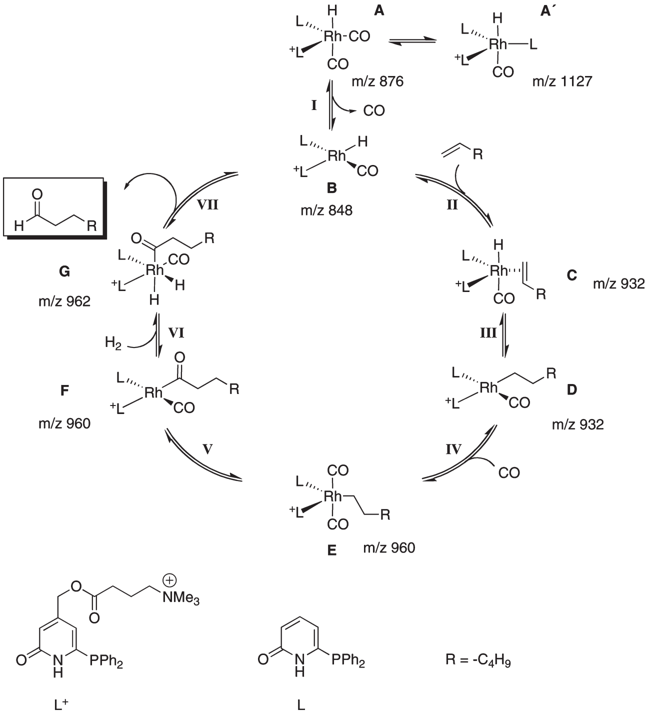

---

(6) Williams, V. M.; Rock Kong, J.; Joon, Ko, B.; Mantri, Y.; Brodbelt, J. S.; Baik, M.-H.; Krische, M. J. *J. Am. Chem. Soc.* **2009**, *131*, 16054.

(7) Breit, B. *Angew. Chem.* **2005**, *117*, 6976. *Angew. Chem., Int. Ed.* **2005**, *44*, 6816. Breit, B.; Seiche, W. *J. Am. Chem. Soc.* **2003**, *125*, 6608.

(8) For alternative approaches to bidentate ligands through self-assembly, see ref 6 and: (a) Takacs, J. M.; Reddy, D. S.; Moteki, A.; Wu, D.; Palencia, H. *J. Am. Chem. Soc.* **2004**, *126*, 4494. (b) Wilkinson, M. J.; van Leeuwen, P. W. N. M.; Reek, J. N. H. *Org. Biomol. Chem.* **2005**, *3*, 2371. (c) Slagt, V. F.; Röder, M.; Kamer, P. C. J.; van Leeuwen, P. W. N. M.; Reek, J. N. H. *J. Am. Chem. Soc.* **2004**, *126*, 4056. (d) Slagt, V. F.; van Leeuwen, P. W. N. M.; Reek, J. N. H. *Angew. Chem.* **2003**, *115*, 5777. ; *Angew. Chem., Int. Ed.* **2003**, *42*, 5619. (e) Slagt, V. F.; van Leeuwen, P. W. N. M.; Reek, J. N. H. *Chem. Commun.* **2003**, 2474.

(9) (a) Breit, B.; Seiche, W. *J. Am. Chem. Soc.* **2003**, *125*, 6608. (b) Breit, B.; Seiche, W. *Angew. Chem.* **2005**, *117*, 1666. ; *Angew. Chem., Int. Ed.* **2005**, *44*, 1640. (c) Seiche, W.; Schuschkowski, A.; Breit, B. *Adv. Synth. Catal.* **2005**, *347*, 1488. (d) Waloch, C.; Wieland, J.; Keller, M.; Breit, B. *Angew. Chem.* **2007**, *119*, 3097. ; *Angew. Chem., Int. Ed.* **2007**, *46*, 3037.

(10) Chevallier, F.; Breit, B. *Angew. Chem.* **2006**, *118*, 1629. ; *Angew. Chem., Int. Ed.* **2006**, *45*, 1599.

(11) Weis, M.; Waloch, C.; Seiche, W.; Breit, B. *J. Am. Chem. Soc.* **2006**, *128*, 4188.

(12) de Greef, M.; Breit, B. *Angew. Chem.* **2009**, *121*, 559.

(13) (a) Mohr, B.; Lynn, D. M.; Grubbs, R. H. *Organometallics* **1996**, *15*, 4317. (b) Hinderling, C.; Adhlart, C.; Chen, P. *Angew. Chem., Int. Ed.* **1998**, *37*, 2685.

Scheme 8. ESI-MS Spectrum of the **10**/**1**/[Rh(CO)$_2$acac] Mixture under a CO/H_2 Atmosphere

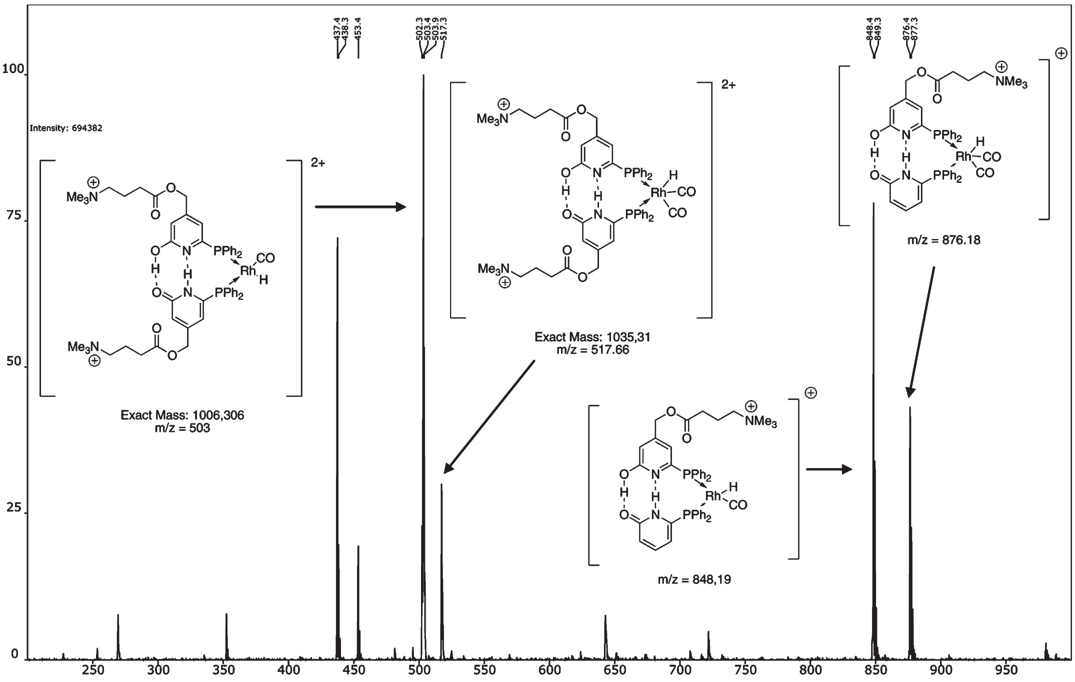

Scheme 9. ESI-MS Spectrum of the Proposed Resting State A′

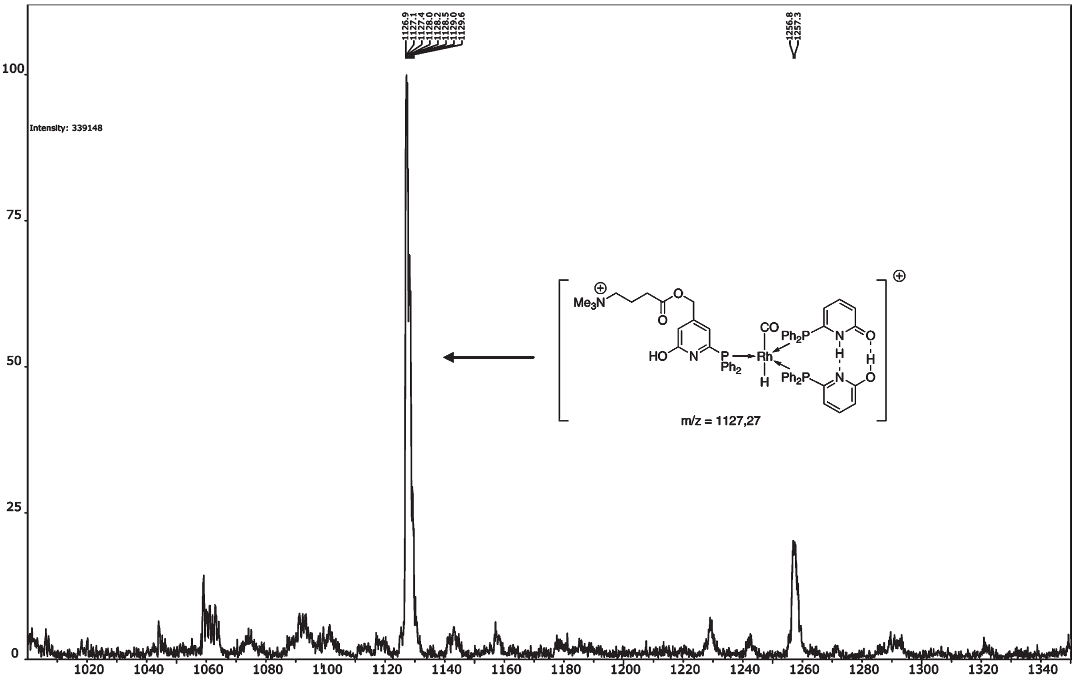

should exhibit a much higher ionization tendency than negatively charged groups. The complete synthesis toward the final ligand **10** is depicted in Scheme 2, and detailed experimental data and spectra are given in the Supporting Information.

ESI-MS investigation of a CH_3CN solution of **10** confirmed the purity and the high ionization tendency of the charged ligand, as anticipated (Scheme 3).

Comparison of the Performance of 10 and 6-DPPon (1) in the Course of the Rhodium-Catalyzed Hydroformylation. To test the ability of ligand **10** to form bidentate metal ligand complexes, a [PtCl$_2$(ligand)$_2$] complex was generated *in situ* and studied by ^{31}P and ^{1}H NMR spectroscopy. The resulting P,Pt coupling constant can provide an indication about the structure of the formed complex, with coupling constants greater than 3000 Hz suggesting a *cis* arrangement of the ligands. Furthermore, the formation of stabilizing hydrogen bonds can be monitored in the proton NMR, normally as a pair of signals at around δ 10−12 ppm.

Thus, PtCl$_2$(COD) was mixed with 2 equiv of **10** in CD_3CN and investigated by ^{31}P/^{1}H NMR spectroscopy. The resulting spectra, depicted in Schemes 4 and 5, clearly show the formation of a [PtCl$_2$(**10**)$_2$] complex (the obtained P,Pt coupling constant of $J_{P,Pt}$ = 3645.78 Hz indicates a *cis* configuration), which corresponds to structure **11** and is in good agreement with the results obtained for the parent system [PtCl$_2$(6-DPPon)$_2$].[9]

In the ^{1}H NMR, the two hydrogens involved in hydrogen bonding show a resonance at δ = 12.1 ppm. The two distinct

Scheme 10. CID Experiment of *m*/*z* 1127

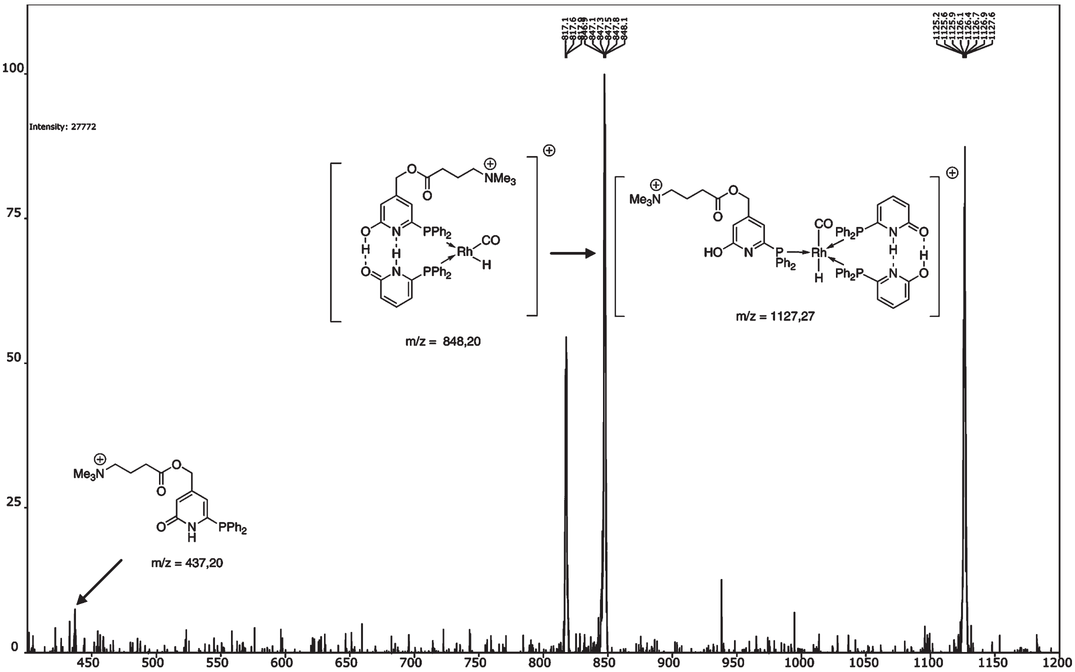

signals normally observed coincide to a broad signal with the intensity of two protons, probably due to solvent effects.

To make sure that the ammonium-functionalized new monodentate ligand **10** and the parent 6-DPPon system **1** display similar self-assembling properties in catalysis, we studied both systems in the course of the Rh-catalyzed hydroformylation employing 1-octene as a prototype for a terminal alkene (Table 1).

Due to solubility reasons, the reactions were carried out in CH_3CN as a solvent, which surprisingly did not influence the catalyst performance with regard to selectivity or reactivity (see entry 4 for a reaction in toluene that has been employed as the standard solvent previously[9]). It is known that polar solvents degrade the performance of these catalysts with regard to both activity and selectivity.[14]

In all cases, conversion was quantitative after 20 h. The obtained selectivities for the linear product were excellent for both the cationic system **10** and 6-DPPon (**1**) and clearly indicate the formation of a pseudo-bidentate catalyst system in all cases. Furthermore, also when applying a 1:1 mixture of charged and uncharged ligand, the observed high regioselectivity indicates the formation of a self-assembling ligand system (Table 1, entry 3). In conclusion, no difference could be observed between 6-DPPon (**1**) and the new cationic derivative **10**.

ESI-MS Investigations. To shed some light on the mechanism of the hydroformylation reaction, several steps were examined. First, the catalyst precursor complex resulting from mixing the ligand and $[Rh(COD)_2]BF_4$ was electrosprayed to assess the complexity of the ion mixture; afterward online monitoring of the reaction medium under hydroformylation conditions (both with and without substrate) was performed.

Thus, a CH_3CN solution of the catalyst precursor generated *in situ* upon mixing 4 equiv of cationic ligand **10** and 1 equiv of $[Rh(NBD)_2]BF_4$ was investigated by ESI-MS, revealing a much more complex mixture of ions than expected (Scheme 6 and Supporting Information).

Most of these ions have not been detected by other methods before. IR and NMR experiments normally only show a single complex that is thought to be a resting state containing three ligands. ESI-MS experiments show, among other ions, a complex consisting of Rh^+ and two ligands to be the predominant species. The rest of the ion population includes multiple charged species, species containing counterions, singly charged species due to deprotonation, and free uncoordinated ligands. This mixture is partially the result of the processes that take place during droplet shrinkage right after electrospray. Due to the difference in environment provided by the droplet and the gas phase, multiply charged ions present in the droplets engage in energetically favorable processes that lead to net charge reduction: intra- and intercluster H^+ transfers, the transfer of a proton between two ions, and binding of a counterion.[15] These unavoidable processes complicate the acquired spectra.

Scheme 11. X-ray Structure of 15

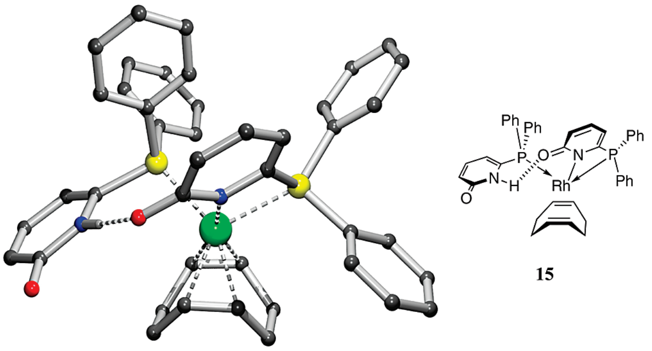

15

To reduce this complexity, several mixtures of charged ligand **10** and uncharged ligand **1** were studied. After extensive experimentation it was found that applying a mixture of cationic ligand **10** and neutral 6-DPPon (**1**) in a 1:1 ratio in the presence of 1 equiv of the Rh precursor provided less complex spectra while in the hydroformylation reaction maintaining high catalytic activity and selectivity.

A closer look into these spectra shows no obvious candidates for some of the species postulated in the Wilkinson cycle, as expected because of the absence of synthesis gas, thus prompting further experiments under hydroformylation conditions.

---

(14) (a) See ref 8a and: (b) Waloch, C.; Wieland, J.; Keller, M.; Breit, B. *Angew. Chem., Int. Ed.* **2007**, *46*, 3037 for hydroformylation in polar solvents applying different heteroaromatic platforms.

(15) Kebarle, P.; Yeughaw, H. O. In *Electrospray Mass Spectrometry*; Cole, R. B., Ed.; J. Wiley & Sons: New York, 1997; Chapter 1.

Scheme 12. CID Experiment with *m*/*z* 848

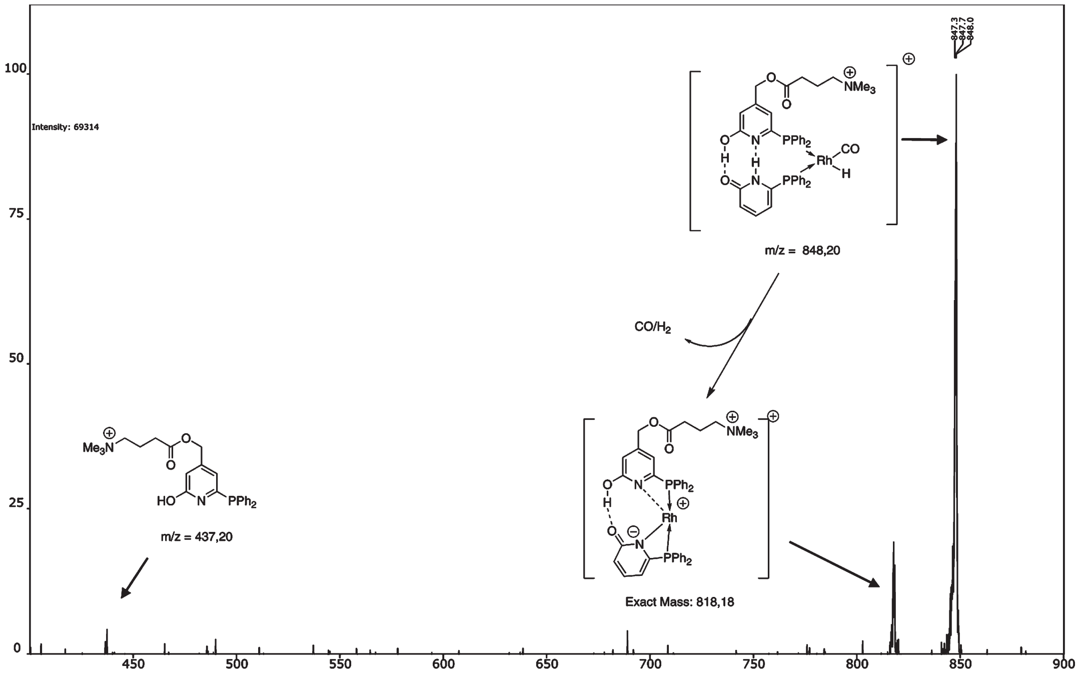

Scheme 13. CID Experiment with *m*/*z* 848 under CO/D$_2$

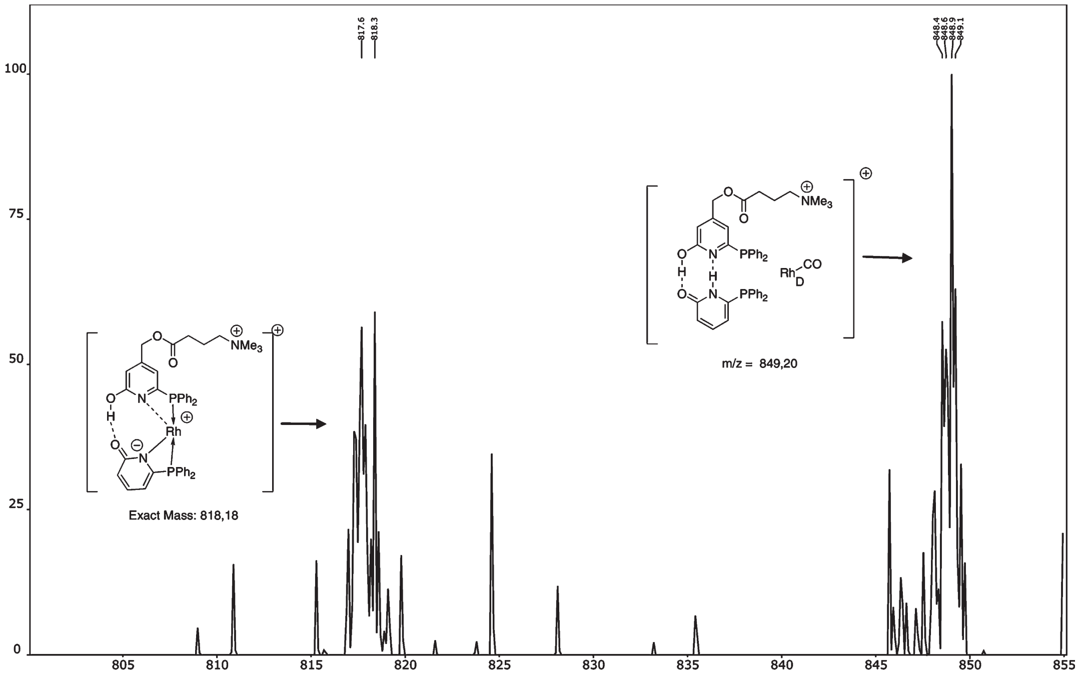

Live Streaming. The next logical step was to live stream reaction media into the mass spectrometer using the techniques developed for that end. The above-mentioned mixture was subjected to a CO/H$_2$ atmosphere (20 bar) in a stainless steel autoclave equipped with a capillary connected directly to the ESI-MS. The pressure inside the autoclave pushes the analyte mixture all the way through the pipe to the electrospray tip of the MS, and a pair of split valves regulate the flow, as described elsewhere.[3]

Under these conditions several new complexes are anticipated to be present corresponding to the intermediates **A**, **A′**, and **B** in the commonly accepted catalytic cycle proposed by Wilkinson,[16] Heck, and Breslow,[17] as shown in Scheme 7.

Without substrate present in the reaction mixture, several ions containing CO and H$_2$ could be detected, *m*/*z* 848, *m*/*z* 876, and the "resting state" *m*/*z* 1127. In addition, the corresponding complexes derived from two charged ligands are present also (*m*/*z* 503 and 517), as depicted in Scheme 8. The assignment of the molecular structures is based on CID experiments, i.e., collision of the parent ion with an inert gas at different collision energies and monitoring of the resulting fragments (daughter ions).

---

[16] Evans, D.; Osborn, J. A.; Wilkinson, G. *J. Chem. Soc. A* **1968**, 3133.

[17] (a) Heck, R. F.; Breslow, D. S. *J. Am. Chem. Soc.* **1961**, *83*, 4023. (b) Heck, R. F.; Breslow, D. S. *J. Am. Chem. Soc.* **1962**, *84*, 2499.

Scheme 14. CID Experiment with *m*/*z* 848 and CO As Collision Gas

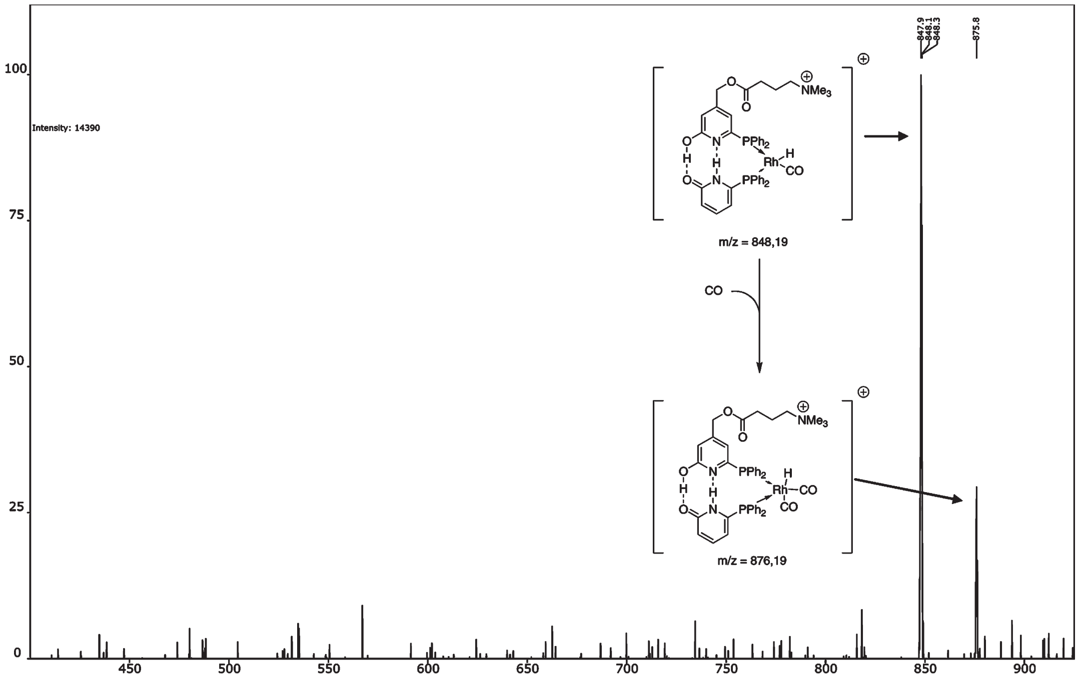

Scheme 15. Alternative Structure for B (right side)

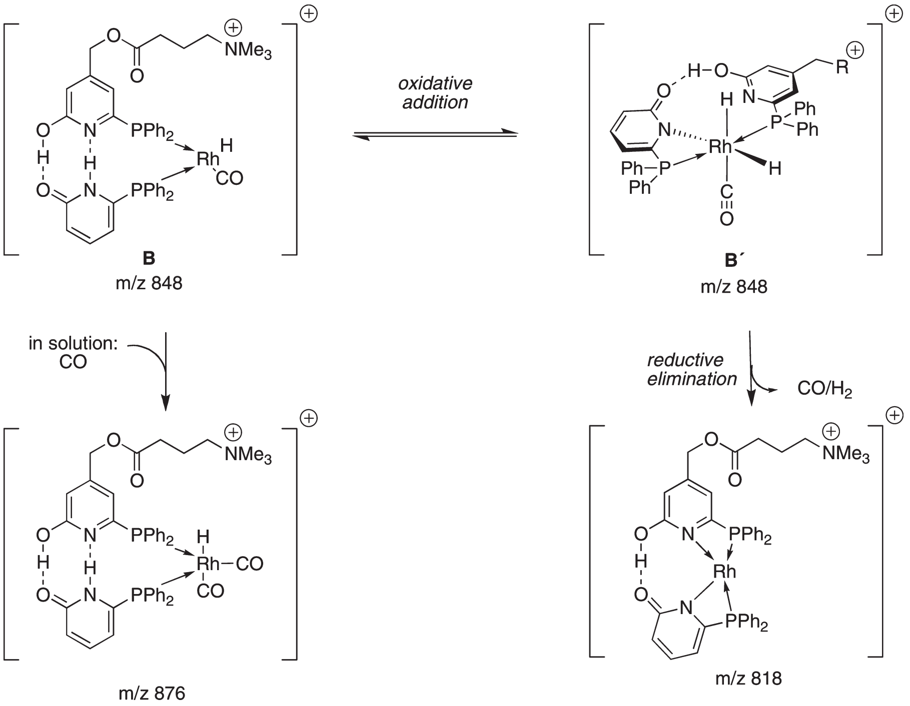

The structure of the resting state (*m*/*z* 1127), which has been described with 6-DPPon before and affirmed by X-ray analysis, was tested in CID experiments. Using argon as collision gas this ion yields several fragments, an ion with *m*/*z* 848 resulting from the loss of one 6-DPPon ligand and *m*/*z* 437, which corresponds to **10**, thus suggesting the assumed structure **A′** (Scheme 10).

To our surprise, a very prominent ion of *m*/*z* 818, which corresponds to [Rh(6-DPPon)(**10**)(-H)]$^+$, is always present. This ion has not been previously spotted using other techniques. A complex that might be comparable in structure could be prepared upon reaction of 6-DPPon and [Rh(COD)acac]. X-ray analysis revealed the structure depicted in Scheme 11.

One pyridone has lost a proton, resulting in a strong tridentate P,N,P coordination motif. Such a coordination mode could also be present in the detected ion at *m*/*z* 818, making it more sterically compromised, or even occupying all coordination sites, rendering it unreactive.

In addition to the analytical detection of solution-phase intermediates, ESI-MS can provide information about the structure and reactivity of these intermediates by conducting gas-phase ion−molecule reactions of the species of interest with suitable reactants.[1,2]

When reacting the ion at *m*/*z* 818 with Ar, D_2, CO, olefins, or aldehydes in the gas-phase at different collision energies and

Scheme 16. CID with *m*/*z* 960

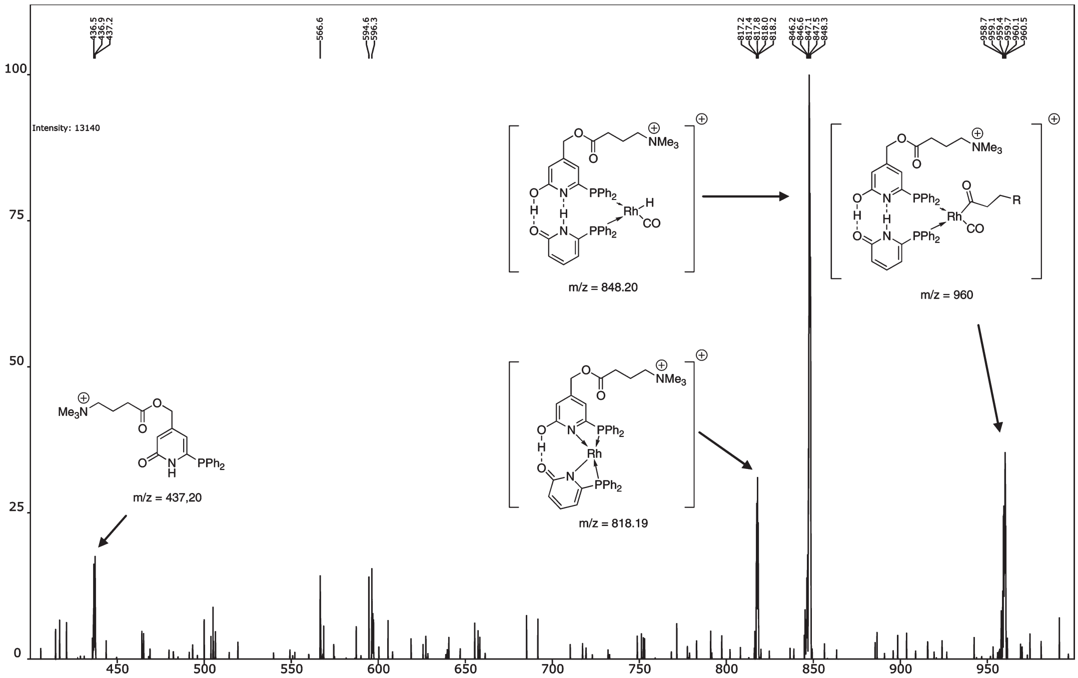

pressures, no new signals could be detected other than the fragments already mentioned.

Furthermore, the ion at *m*/*z* 848 (**B**), which represents the starting point of the catalytic cycle and is normally not detectable in solution, was of special interest and investigated further by means of CID experiments in the gas phase.

Upon CID, this ion loses 30 mass units to produce an ion of *m*/*z* 818 or loses 511 *m*/*z* units to produce an ion of *m*/*z* 437 that corresponds to **10** (see Scheme 12).

Assignment of this species (the hydridocarbonyl complex) is confirmed by an experiment using D_2 instead of H_2. The mass shift of the corresponding species **B**-d_1 is +1 (Scheme 13). Consequently the fragmentation pathway leading to the loss of CO and H_2 becomes the loss of CO and HD by CID of **B**-d_1. The mechanistic interpretation of this fragmentation will be discussed in detail below.

By those observations we concluded that the structure of the ion at *m*/*z* 848 is indeed **B** in the cycle above (Scheme 7). To get more information about the true nature of the complex, it was reacted with CO as collision gas, producing an ion at *m*/*z* 876 in very low yield and only at low collision energies (0 to 6 eV (lab scale), Scheme 14) that is also spotted when synthesis gas is present and represents **A** (*vide supra*). No further fragments are created at higher energies. Upon reaction with olefins, no adducts are detected and fragmentation seems to be the only pathway.

As the unsaturated complex **B** should have a square-planar geometry with free coordination sites, this lack of reactivity seems unlikely. Bearing the observed loss of H_2 in mind, one could envision a modified structure of **B** that results from an oxidative addition of the N−H part of the hydrogen-bond framework. This indeed could be the case here, as some preliminary DFT calculations of the parent system complex [HRh(CO)(6-DPPon)$_2$] indicate that the OH−O bond is much stronger than the NH−N bond, the latter opening up to a great extent in the course of the catalytic cycle, thus making it accessible for the proposed oxidative addition (Scheme 15).

In solution, as depicted on the left side of Scheme 15, the species **B** would react immediately with either additional ligand or a CO molecule, forming the saturated species *m*/*z* 876. However, this pathway is not accessible in the gas phase, as no uncharged reaction partners are present. The assumed structure **B′** indeed could explain the observed lack in reactivity when using olefins as collision gas, as no free coordination sites are present. *Syn* eliminiation of H_2 would be feasible from **B′**, followed by loss of CO (or the other way around), giving the complex with *m*/*z* 818, which is observed regardless of the kind of collision gas used.

Scheme 17. Possible Complex E′ and Fragmentation Pattern of *m*/*z* 960

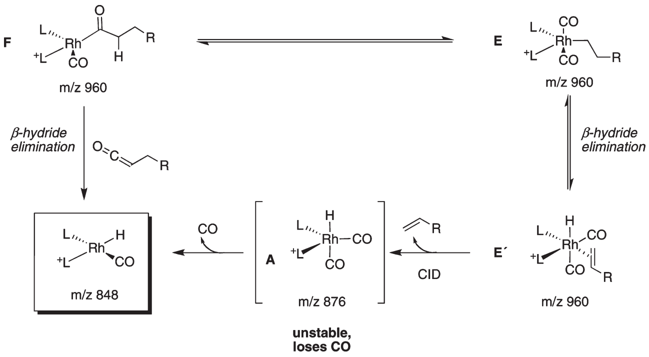

Reactions with Substrate in the Mixture. After the successful identification of crucial intermediates of the catalytic cycle (**A**, **A′**, **B**), the next logical step was to analyze a mixture under bona fide hydroformylation conditions, i.e., in the presence of an olefinic substrate. We decided to use 1-hexene, as it reacts quite readily under the applied conditions.

In first experiments, we applied standard hydroformylation conditions ([Rh]:L1:L2:1-hexene = 1:1.1:1.1:100, CO/H_2 = 1:1, 20 bar, CH_3CN, *c*(1-hexene) = 0.36 M). However, no new ions could be detected. Hence, either the steps in the catalytic cycle are faster than our time frame or the concentrations of the species of interest lie below the detection limit of the method. Indeed, when increasing the amount of substrate to a concentration of 50 vol % of 1-hexene, a possible acyl complex at *m*/*z* 960 (**E** or **F**) could be detected and further investigated. Additionally, an ion of *m*/*z* 932 (**C** or **D**) was present too, but the low intensity of the signal disallowed CID experiments.

Upon CID with Ar or D_2, the ion at *m*/*z* 960 reveals several interesting fragments, namely, *m*/*z* 848, which could be **B** in the catalytic cycle, and *m*/*z* 818. No ions such as *m*/*z* 932 (**C** or **D**),

Scheme 18. ESI-MS Spectra under CO/D_2 Atmosphere and with Substrate in Solution[a]

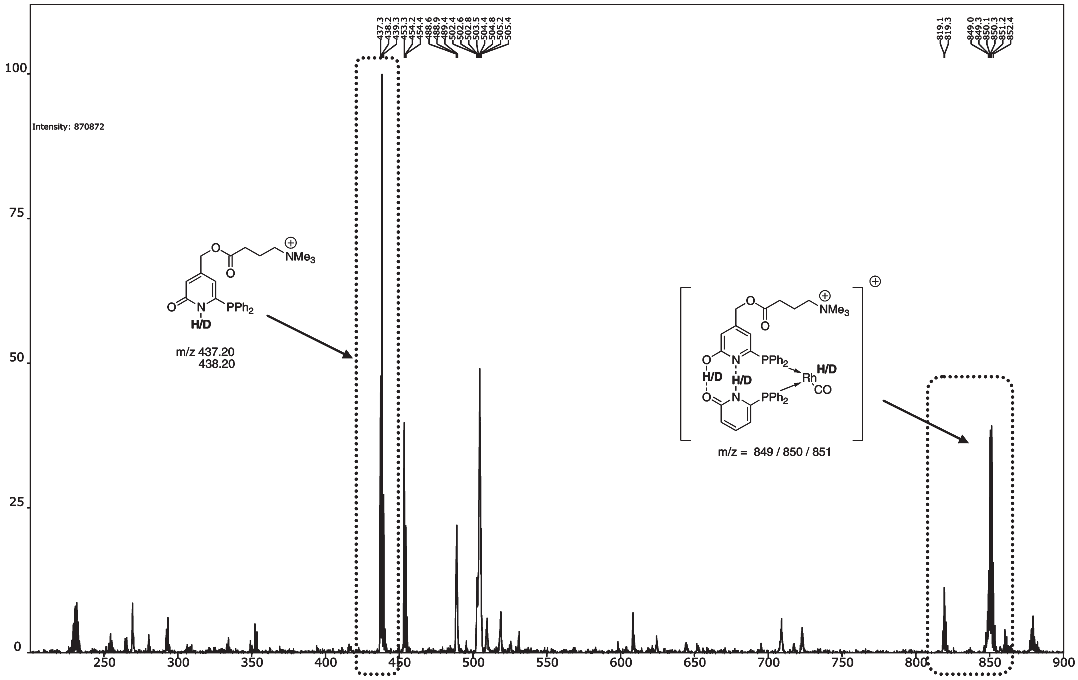

[a] Highlighted areas are shown in Schemes 19 and 20.

Scheme 19. ESI-MS Spectra under CO/D_2 Atmosphere and with Substrate in Solution (*m*/*z* 750 to 860)

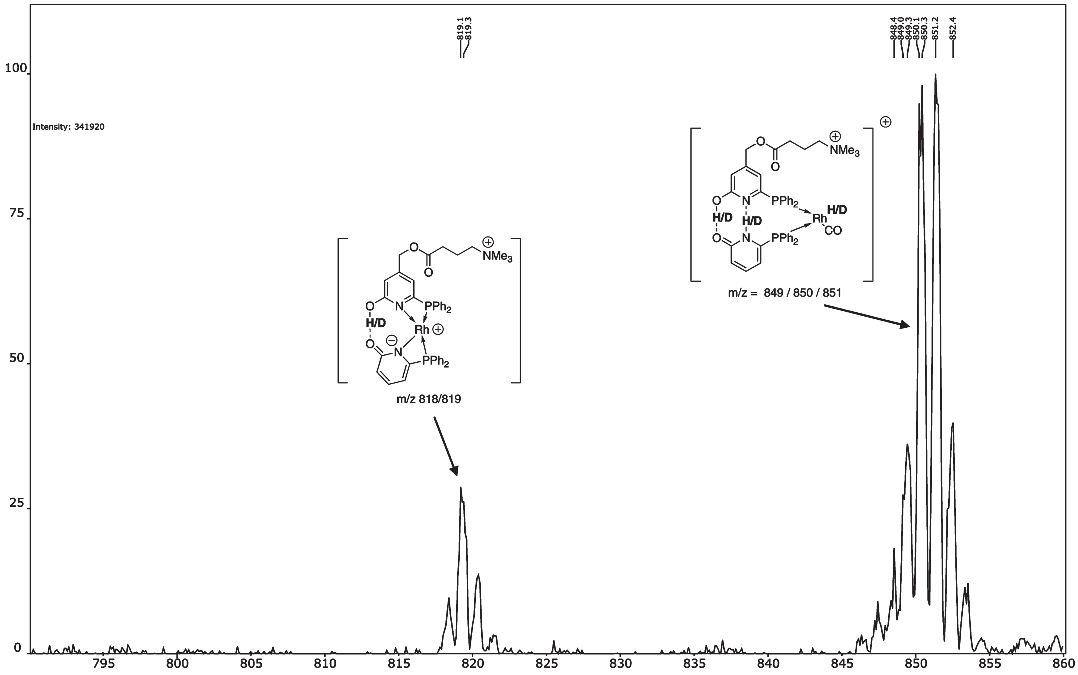

where one CO is lost, or *m*/*z* 876 (**A**), where only the unreacted olefin is lost, were detected (Scheme 16).

An ion equivalent to *m*/*z* 960 but at *m*/*z* 980 is present when an excess of styrene is used instead of 1-hexene, but its signal proved too weak for further CID experiments. Styrene is thought to form a stable acyl complex with Rh under hydroformylation conditions, proved by NMR studies.[18]

The structure of *m*/*z* 960, which should correspond to **E** or **F**, should react with D_2 to regenerate **A** + 1 *m*/*z* unit. However, it failed to do so in our experiments. Furthermore, it reacts in the same manner, giving *m*/*z* 848 with Ar as collision gas, where only fragmentation would be expected. One logical conclusion for this unexpected reactivity is that the structure of *m*/*z* 960 resembles neither the proposed complex **E** nor **F**. Instead, one could think of the olefin complex **E′** resulting from *β-hydride elimination* (see Scheme 17).

Colliding **E′** with any collision gas would result in the loss of the weakly bound olefin ligand, giving *m*/*z* 876, which is **A** in Scheme 7. As shown before (Scheme 14), this complex is stable only under very low collision energies, instantaneously losing the second CO molecule, giving *m*/*z* 848. Alternatively, a direct

---

[18] Brown, J. M.; Kent, A. G. *J. Chem. Soc., Perkin Trans. 2* **1987**, 1597.

Scheme 20. ESI-MS Spectra under CO/D_2 Atmosphere and with Substrate in Solution (*m*/*z* 430 to 450) after 20 min (left) and 2 h (right) Reaction Time

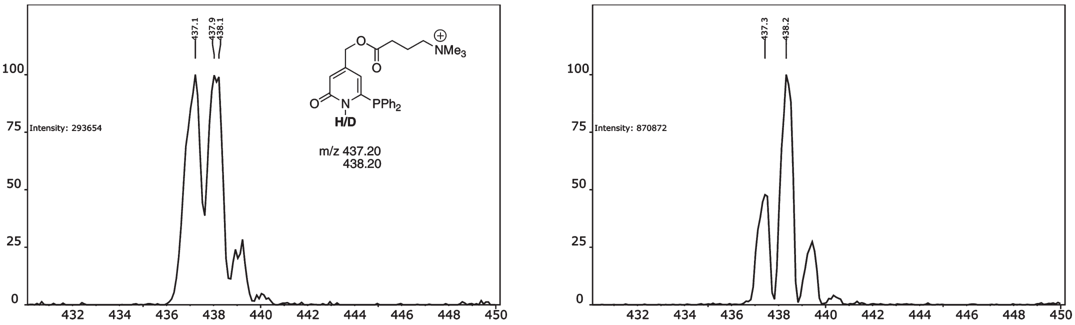

Scheme 21. Proposed Pathway for the D_2 Incorporation in 10

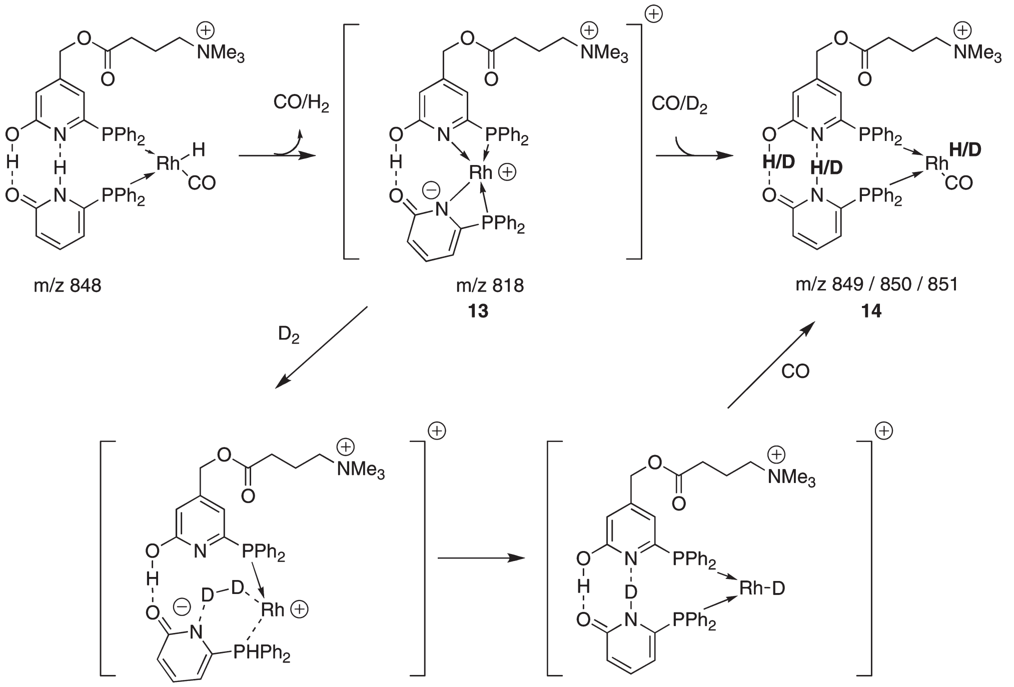

β-hydride elimination from **F**, liberating a ketene, would result directly in the complex *m*/*z* 848 (Scheme 17, left side). Although a reaction like this seems unlikely and has not been reported for Rh complexes, there is evidence for the elimination of a ketene from comparable Ru complexes [Ru(COMe)$(CO)_2$-(triphos)]Cl.[19]

D_2-Incorporation Experiments. Using D_2/CO as synthesis gas gave more insight into the nature of the ion at *m*/*z* 848 and the catalytic cycle itself. When no substrate is present, only one deuterium atom is incorporated to **B**, shifting its mass up one *m*/*z* unit. Upon collision, 31 or 30 *m*/*z* mass units were lost. Incorporation of deuterium was not complete, and thus only a part of the ion population at *m*/*z* 849 had a deuterium atom bound to the Rh center. The ion corresponding to **10** was detected at *m*/*z* 437 and 438 (see above).

Adding a substrate proved revealing. While the main mass shift for **B** was 2 mass units (Scheme 18) and upon collision the same behavior as before was seen, the free ligand was detected as a mixture of ions with *m*/*z* 437 and 438 (Scheme 20).

This finding clearly points to the involvement of the H atoms of the hydrogen-bond framework into the catalytic cycle, as turnover seems to be crucial for the observed incorporation of deuterium into the ligand. This incorporation is progressive, as the right spectrum in Scheme 20 was taken two hours after the start of the reaction, reaching approximately a 2:1 ratio for heavy versus normal.

To explain the observed deuteration, two different pathways seem to be reasonable; the first one, being more closely related to the commonly accepted catalytic cycle, is depicted in Scheme 21.

After loss of CO and H_2 a complex with P,N,P or even double P,N coordination results that partially resembles the structure being identified by X-ray (see Scheme 11). The close and stable P,N coordination might be the reason for the lack of reactivity in our gas-phase investigations. In solution, on the other hand, due to the presence of a vast variety of competing coordinating agents (CO, solvent molecules, abundant ligand), one might envision a weaker bonding of the ligands. Activation of deuterium or hydrogen can take place over a thermodynamically preferred six-membered transition state, resulting in the incorporation of deuterium into the ligands, as observed. CO coordination regenerates in the last step the now deuterated complex **14**.

The second pathway we like to propose is based on the above-mentioned *oxidative addition* step possible for complex **B**, giving rise to a new mechanism (Scheme 22).

The intermediate **F** could undergo an oxidative addition yielding the Rh(III) complex **F′**, followed by reductive elimination to

---

[19] Hommeltoft, S. I.; Baird, M. C. *J. Am. Chem. Soc.* **1985**, *107*, 2548.

Scheme 22. Proposed New Hydroformylation Mechanism for Self-Assembling Ligands

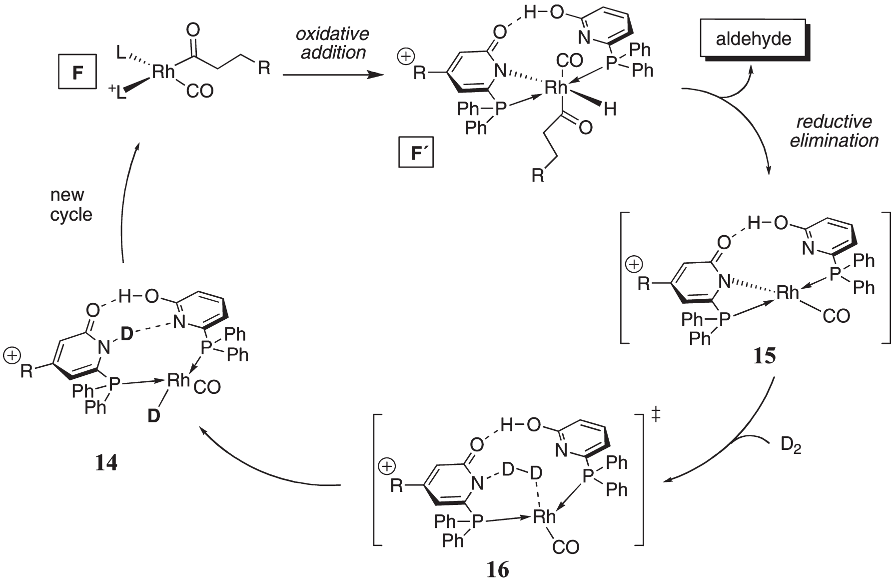

liberate the product aldehyde. The resulting complex **15** can be seen as structurally related to **13** in Scheme 21, having one more CO ligand. H_2/D_2 activation can proceed also over a six-membered transition state (**16**), regenerating the now deuterated complex **14**, which enters a new catalytic cycle. This unprecedented catalytic cycle would not only explain the observed incorporation of deuterium into the free ligand but explain why we never detected a complex **G** that would be the result of oxidative addition of hydrogen: if the hydroformylation reaction applying our self-assembling ligands could indeed proceed in the above depicted way, a complex **G** with *m*/*z* 962 simply would not occur.

Nonetheless, at this point we cannot comment on the possibility of these mechanistic pathways being by any means part of the catalytic cycle of the hydroformylation itself in solution and not only an orthogonal equilibrium phenomenon. The unique nature of our self-assembling ligand systems and the highly dynamic tautomeric behavior of the applied 6-DPPon ligand could be the basis for this unprecedented reactivity. These findings seem to be in accordance with literature examples where a similar involvement of two hydrogen atoms—one at the metal center, another at a heteroatom—occurs.[20,21]

Further investigations, especially with our other heterobidentate self-assembling ligands, together with quantum mechanical calculations to further affirm the observed phenomena, are ongoing and will help to shed more light on the mechanism of the hydroformylation and other transition-metal-catalyzed reactions.

Acknowledgment. This work was supported by the DFG, the International Research Training Group "Catalysts and Catalytic Reactions for Organic Synthesis" (IRTG 1038), and the Alfried Krupp Award for young university teachers (to B.B.). We thank Günther Leonhardt-Lutterbeck for great technical assistance.

Supporting Information Available: This material is available free of charge via the Internet at http://pubs.acs.org.

---

(20) Casey, C. P.; Singer, S. W.; Powell, D. R.; Hayashi, R. K.; Kavana, M. *J. Am. Chem. Soc.* **2001**, *123*, 1090, and references therein.

(21) Yamakawa, M.; Ito, H.; Noyori, R. *J. Am. Chem. Soc.* **2000**, *122*, 1466.